

2D fractal analysis of synfolding fractures in the Khushalgarh area, eastern Kohat plateau, northern Pakistan

MOHAMMAD SAYAB¹, QAUID K. JADOON², GHAZANFAR A. KHATTAK¹
& SAQIB PARACHA³

¹National Centre of Excellence in Geology, University of Peshawar

²LMK Resources, ETC building, Sir Agha Khan Road, F-5/1, Islamabad

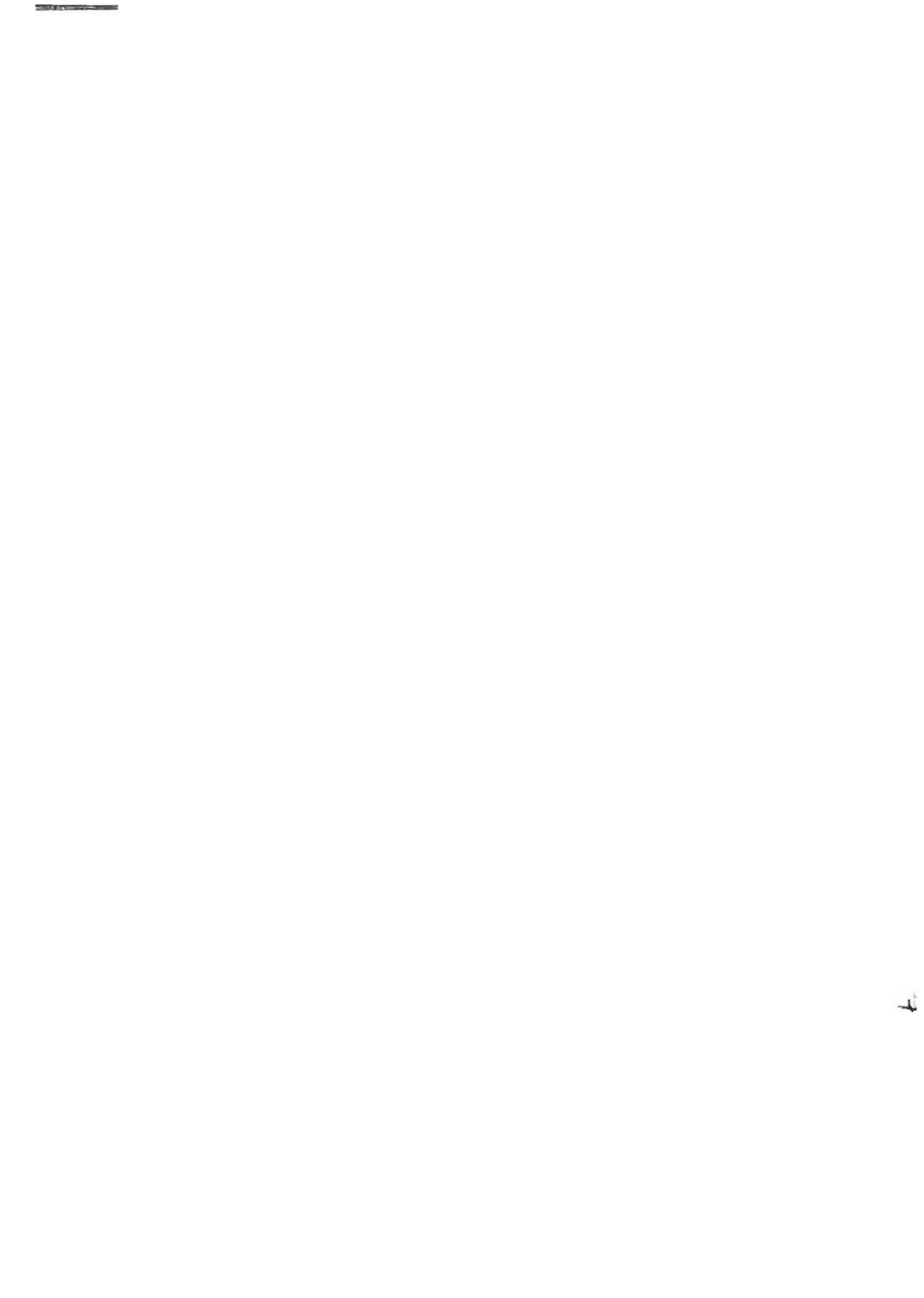
³Department of Geology, University of Peshawar

ABSTRACT: *Outcrop data has been used to investigate the spatial distribution of fracture system that has affected the Miocene Kamliyal Formation of the Khushalgarh syncline from foreland area of the Pakistani Himalaya. The fracture system is dominated by near-orthogonal network of NE-SW and NW-SE striking fractures. The NE-SW fractures follow the axis of the syncline, whereas NW-SE fractures crosscut the fold axis. The scaling properties of these fracture system are analyzed from high quality, outcrop scale digital photographs of two locations, A and B. After digitization of fractures on commercially available drawing software, 2D binary images were prepared for standard box-counting technique. The fracture sets are considered as a whole and not as an individual set of fractures. The results show that the spatial distribution of fractures and their growth follow power-law with fractal dimension (D) at location A ($D = -1.153 \pm 0.057$) and B ($D = -1.156 \pm 0.050$), and have upper and lower fractal limit. The D values are effectively identical with minimum standard errors. The results conclusively suggest that there is a genetic link between the fractures from one location to another and that they developed synchronous with the folding event. The results have important implications on the geometry and growth propagation of the fracture development during folding, where the fracture sets are interpreted as tectonic in origin and are synchronous with the post-Miocene folding of the Kamliyal Formation and are not pre- or post-folding fractures.*

INTRODUCTION

Geological fractures are discontinuous structures or discrete breaks within a rock mass that develop in response to stress. Fractures include faults, across which shear displacement occur; joints, which have an aperture but show no significant shear displacement, and filled structures, such as veins. They exist on a wide range of scales from microns to several hundreds of kilometers, and through out this scale range, fractures have a significant effect on crustal

processes including fluid flow (e.g. hydrology and petroleum systems) and rock mechanics (e.g. slope stability) (see Barton & La Pointe, 1995; Turcotte, 1997). Conventional fracture analysis has typically been limited to the orientation distribution of fractures, for example, rose patterns, histograms and stereoplots. However, these techniques provide no significant information regarding their spatial distribution at different scales (see Gillespie et al., 1993). In recent years, it has been suggested that various techniques of fractals may usefully be applied



dipping towards the east and south, respectively. The fractures are slightly undulating and their ends are either connected or abut against the younger

fractures. It is apparent from the outcrop that most of these fractures correspond to shear or mode II fractures.

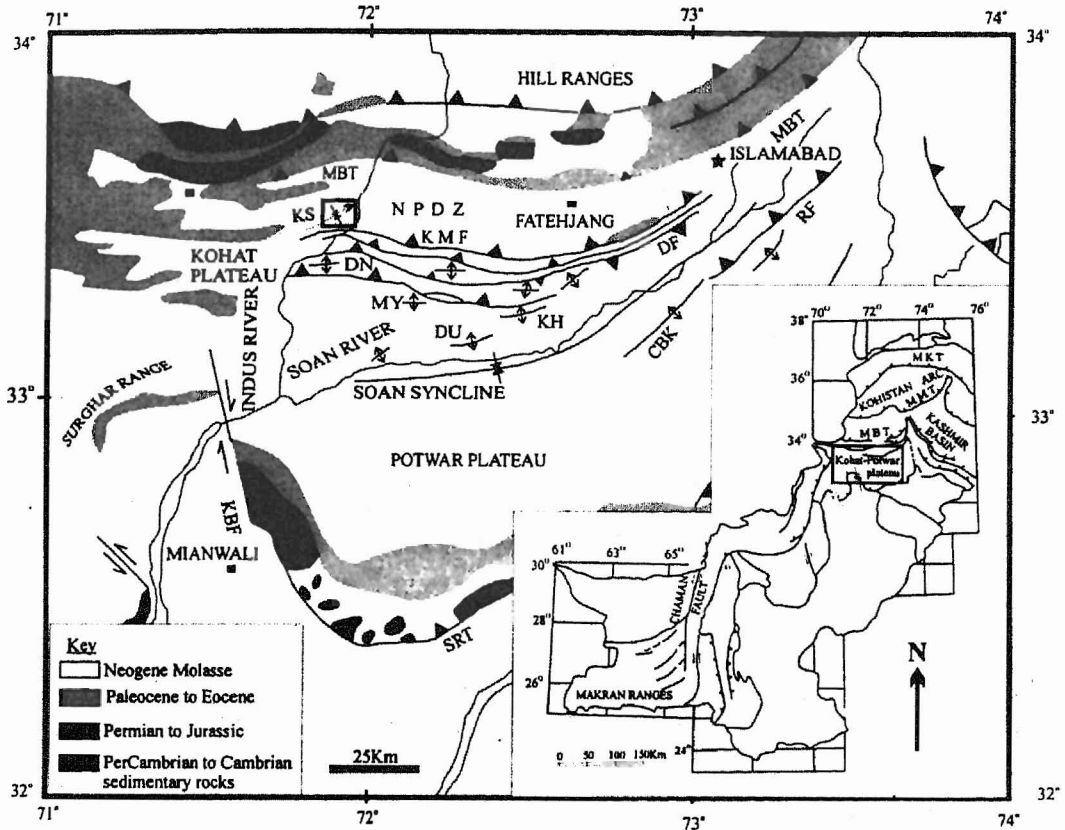


Fig. 1. Generalized map of the Kohat, Potwar and Salt Range showing prominent tectonic features (after Jaswal et al., 1997). KS (Khushalgarh syncline (after Searle and Khan, not dated). CBK = Chak Beli Khan anticline, DF = Dhurnal Fault, DJ = Dil Jabba Fault, DN = Dakhni anticline, DU = Dhulian anticline, KBF = Kalabagh Fault, KH = Khaur anticline, KMF = Kheri Murat Fault, MBT = Main Boundary Thrust, MY = Meyal anticline, RF = Riwat Fault, SRT = Salt Range Thrust

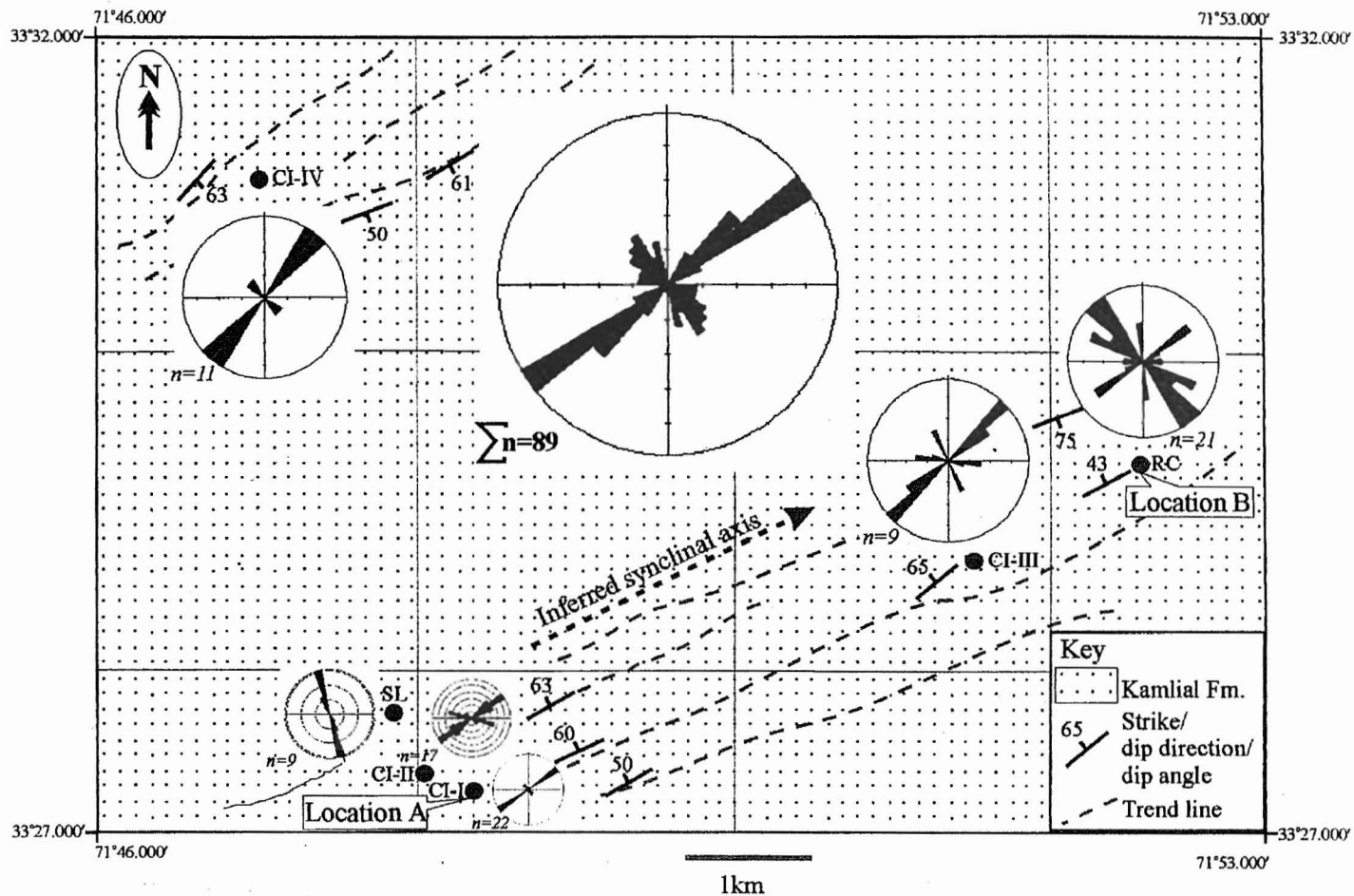


Fig. 2. Fracture pattern in the Kamlial Formation of the Khushalgarh syncline (after Sayab & Jadoon, in review). Note, that the NE-SW fractures follow the axis of the fold, whereas NW-SE fractures cut fold axis at high angle. Inferred fold axis is after Searle & Khan (not dated). CI: circle inventory, SL: scanline, RC, rectangle.

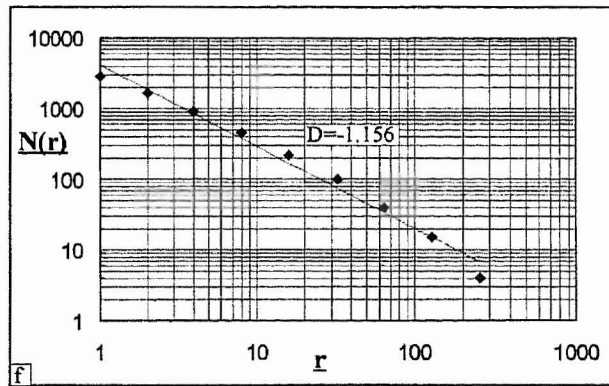
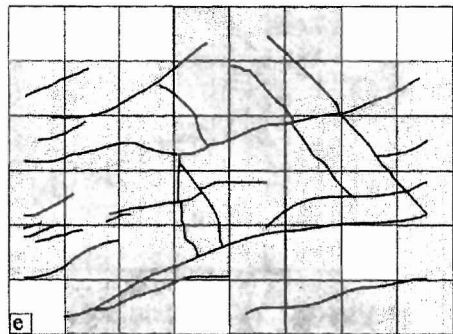
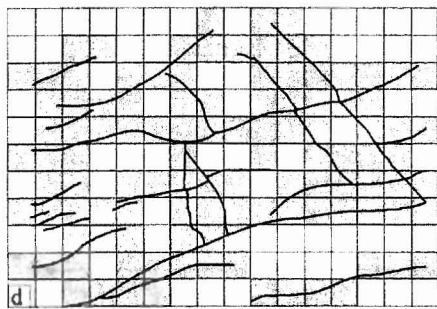
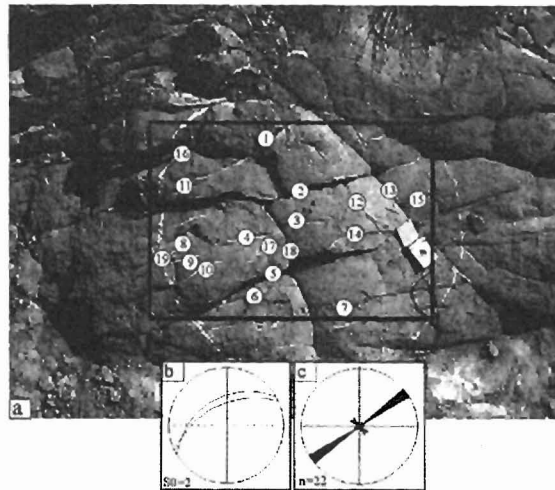
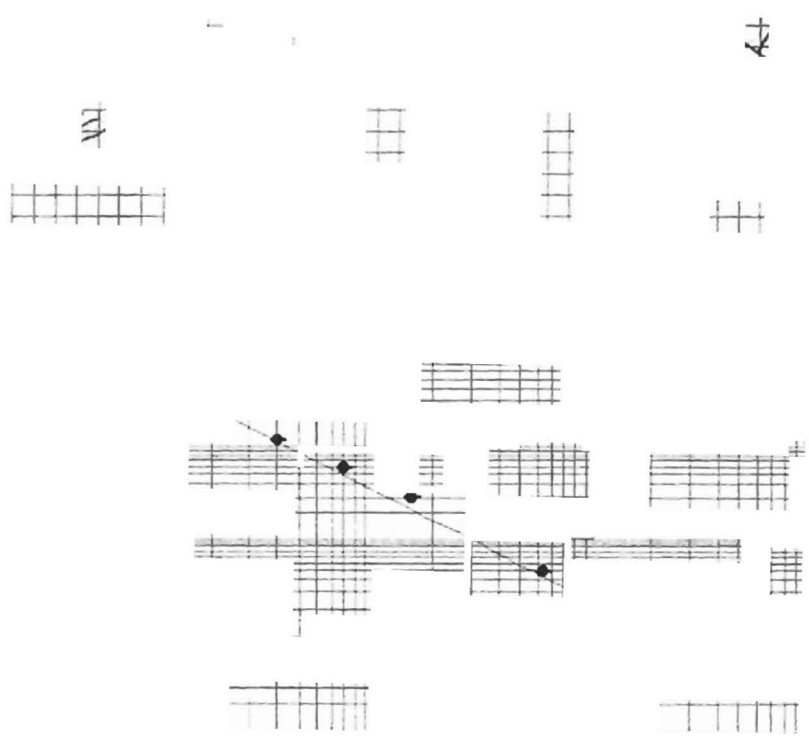
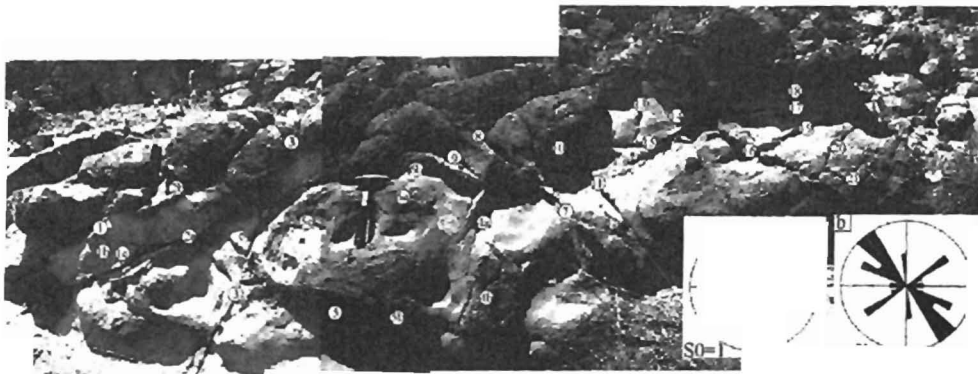


Fig. 3 (a) Fracture pattern from location A. Fractures are numbered for digitization. (b) Lower hemisphere equal area stereographic plot of S_0 . (c) Rose diagram showing fracture trends. (d and e) The box counting method for which the system is covered by a regular mesh of size r . Two different mesh sizes are shown, where boxes inside which fractures are present are shaded. (f) Standard Box counting line for fracture patterns with $D=-1.156$.



METHOD

The mathematical theory of fractals is described by Mandelbrot (1982), and more information about fractals is given by Feder (1988) and Falconer (1990). In the case of fracture systems, Bonnet et al. (2001) defined two ways of measuring the fractals of the fracture patterns, (1) as a set of fractures, where each fracture (or fractures of distinct orientation) defines a separate object and (2) as a fractured domain, where the fracture pattern is considered as a whole. In this study, we have preferred and adopted the second case, as all the observed fractures in the Khushalgarh syncline appear to be synchronous with the folding (Sayab & Jadoon, in review).

The box-counting technique

In the box-counting method, the number of boxes of size r , $N(r)$, required to cover the fractal object is counted (Fig. 3d,e) and should vary as:

$$N(r) \sim r^{-D}$$

Thus, by reporting $N(r)$ versus r on a log-log plot, the fractal dimension (D) can be derived as the slope of the straight line. This method has been widely used to measure the fractal dimension of fractures networks (e.g., Mandelbrot, 1982; Hirata, 1989; Cello, 1997). The spatial distribution of fractures were analyzed using binary images of the 2D fracture photomosaics in the program ImageJ. The range of box size over which the data were linear was 2 to 256 units (Table 1). Regression between these two limits was used to derive the fractal dimensions with standard errors of regression.

Procedure

2D digitized fracture maps have been prepared from oriented field photographs. After digitization of fractures on

commercially available drawing software, the fractures are overlaid with a grid of square boxes, where grids of different-size boxes are used (Fig. 3d,e & 4c) The number of boxes N of size r required to cover the fractures is then plotted on log-log graph as a function of r . The process was repeated for a range of values of r . The $N(r)$ versus r show a straight line is relationship on log-log plot. From the slope of the line, applicable fractal dimension is obtained.

RESULTS

The results show that the fractal dimension of fractures at locations A ($D = -1.152$) and B ($D = -1.156$) are effectively identical. Data points on a log-log plot are consistent within standard errors (Table 1). The results conclusively suggest that there is a genetic link between the fractures that are developed during the folding event. It is further suggested that all the tectonic fracture sets are synchronous with the post-Miocene folding of the Kamli Formation and are not pre- or post-folding and their spatial distribution follows power-law scales.

TABLE 1. LOG VALUES FOR NUMBER OF BOXES $N(Y)$ VERSUS BOX SIZE $R(X)$

X	Y
0	3.450249
0.30103	3.221153
0.60206	2.956649
0.90309	2.664642
1.20412	2.342423
1.50515	2
1.80618	1.60206
2.10721	1.176091
2.40824	0.60206

Location A, $D = -1.156$; standard error 0.057

